Transport and magnetic properties of $Fe_{1/3}VSe_2$

2008 J. Phys.: Condens. Matter 20 415212

(http://iopscience.iop.org/0953-8984/20/41/415212)

J. Phys.: Condens. Matter **20** (2008) 415212 (6pp) doi:10.1088/0953-8984/20/41/415212

Transport and magnetic properties of $Fe_{1/3}VSe_2$

C S Yadav and A K Rastogi

School of Physical Sciences, Jawaharlal Nehru University, New Delhi 110067, India

E-mail: shekharjnu@gmail.com and akr0700@mail.jnu.ac.in

Received 16 June 2008, in final form 29 August 2008
Published 16 September 2008
Online at stacks.iop.org/JPhysCM/20/415212

Abstract

Electrical conductivity, thermopower and magnetic properties of Fe-intercalated $Fe_{1/3}VSe_2$ has been reported between 4.2 and 300 K. We observe a first-order transition in the resistivity of the sintered pellets around 160 K on cooling. The electronic properties including the transitional hysteresis in the resistance anomaly (from 80 to 160 K) are found to be very sensitive to the structural details of the samples, which were prepared in different annealing conditions. The thermopower results on the sintered pellets are reported between 10 and 300 K. The magnetic measurements between 2 and 300 K and up to 14 T field show the absence of any magnetic ordering in $Fe_{1/3}VSe_2$. The magnetic moment per Fe atom at room temperature (between 1.4 and 1.7 μ_B) is much lower than in previously reported antiferromagnetic FeV_2Se_4. Furthermore, the Curie constant shows a rapid and continuous reduction and, combined with the high field magnetization result at 2 K, suggests a rapid decrease in the paramagnetic moments on cooling to low temperatures and the absence of any magnetic order in $Fe_{1/3}VSe_2$ at low temperatures.

1. Introduction

The structural, magnetic and optical properties of the complexes of the 3d-metal atom intercalated in the layered compounds of Nb- and Ta-dichalcogenide have been extensively reviewed [1–3]. In these compounds, the transition metal atoms form an ordered 2×2 and $\sqrt{3} \times \sqrt{3}$ hexagonal superstructure for the 25% and 33% intercalation, respectively [4]. The 3d moments are localized and show a large anisotropy of paramagnetic susceptibility, and give magnetic order at temperatures between 20 and 120 K via the RKKY exchange coupling through the conduction electrons—the ferromagnetic one for V, Cr and Mn and the antiferromagnetic order for Co and Ni atoms. For the iron intercalated compounds, diverse magnetic behavior depending on the host lattice and the atomic ordering have been reported [5]. In a recent study, the ferromagnetic compound $Fe_{1/4}TaS_2$ ($T_C = 160$ K) showed extreme anisotropy and sharp switching of magnetization at 3.7 T field and 2 K temperature [6, 7].

Ternary compounds FeV_2S_4, FeV_2Se_4 and $FeTi_2Se_4$ are known to show Cr_3S_4-type layered structure [8]. In these compounds a cation-deficient layer (50% Fe atoms) also alternates with the filled layer containing V or Ti atoms, the same as in the above-mentioned compounds of Nb and Ta. The magnetic properties of these compounds show significantly reduced effective moments between 3.0 and 4.2 μ_B per Fe atom, contrary to 4.9 μ_B as expected for the high spin state of Fe^{2+} [9, 10]. But the antiferromagnetic ordering temperatures T_N in these compounds at 131, 94.5 and 134 K, respectively, remain quite similar to that found in Nb and Ta compounds [9, 10].

In our earlier reports, we have published a detailed study of the structural and electronic properties of Fe_xVSe_2 compositions with x varying between 0 and 0.33 [11, 12]. Here we report the properties of the $Fe_{1/3}VSe_2$ compound and the effect of intercalation ordering in different phases. We observed that the different preparation conditions affect the structural properties considerably. These different phases were obtained by varying annealing conditions in the preparation. We have used low temperature and excess Se pressure for their synthesis in order to avoid self-intercalation of V atoms in our compound.

2. Sample preparation

$Fe_{1/3}VSe_2$ was prepared from the elements by a solid state chemical reaction route in a two-step process. At first FeSe and VSe_2 (with 5% excess Se) were prepared by reacting Fe (99.98%), V (99.995%) and Se (99.95%) in the proper

molecular ratio at 600 °C, inside evacuated sealed quartz tubes. FeSe and VSe_2 were then thoroughly ground and mixed in a 1:3 molar ratio. This mixture thus contains excess Se over $Fe_{0.33}VSe_2$ composition. This was vacuum-sealed in separate evacuated quartz tubes for further reaction at different temperatures of 550 and 700 °C for 5 d. The excess amount of selenium was released at the cold end of the sealed tubes. The reacted charges were ground and pelletized at 5 ton pressure before sintering them at the chosen temperatures. These preparation conditions gave the following samples (i) FVS700: annealed at 700 °C for 15 d, (ii) FVS550A: annealed at 550 °C for 7 d, (iii) FVS550B: annealed at 550 °C for 15 d, and (iv) FVS850Q: annealed at 850 °C for 5 d followed by air quenching.

3. Structure

The x-ray diffraction patterns of our $Fe_{1/3}VSe_2$ samples using Cu Kα radiation are presented in figure 1. For comparison we also show a pattern from VSe_2 that was used for the preparation of our compounds. It can be seen that for the FVS700 sample the pattern is very similar to the parent VSe_2, indicating that in this sample Fe is intercalated without any changes in the structure of the host lattice. We could refine the structural parameter using the GSAS-EXPGUI program for powder x-ray diffraction [13] and were able to ascertain the likely occupancy of the Fe atoms. This routine gave a very good fit of the pattern for the choice of Fe atoms on the 1*b* (0 0 0.5) site positions in the space group $P\bar{3}m1$ (no. 164) of VSe_2 [14, 15]. We thus confirm a random occupancy of the octahedral sites by 33% of Fe atoms in between the layers. The hexagonal lattice parameters and the z parameters of the 2*c* (0 0 $\pm z$) positions of the Se atoms obtained after refining the two structures are as follows:

VSe_2: $a = 3.356$ Å, $c = 6.104$ Å, and $z = 0.2665$, $V = 59.53$ Å^3, $Z = 1$.

FVS700: $a = 3.365$ Å, $c = 6.056$ Å, and $z = 0.2537$, $V = 59.38$ Å^3, $Z = 1$.

In 1T-VSe_2, the exceptionally large c/a ratio of 1.819 means a large trigonal elongation of the Se octahedra surrounding a V atom (the ideal c/a value is 1.633). Our results show that Fe intercalation reduces the c/a ratio considerably. Moreover, this reduction is primarily achieved from the decrease in the thickness ($2cz$) of the individual VSe_2 layers by the positive chemical pressure exerted by intercalated Fe atoms. This is a significant result and may explain the increase in the transition temperature from 110 K in VSe_2 to a higher temperature of 160 K in our Fe-intercalated compounds due to similar reasons as for the effect of the application of external pressure on VSe_2. This transition shift towards higher temperatures in the presence of pressure is explained in terms of the pressure-induced broadening of the 3d bands of vanadium, which reduces the correlation effects among the electrons in a narrow band and enhances the charge density wave (CDW) instability [16].

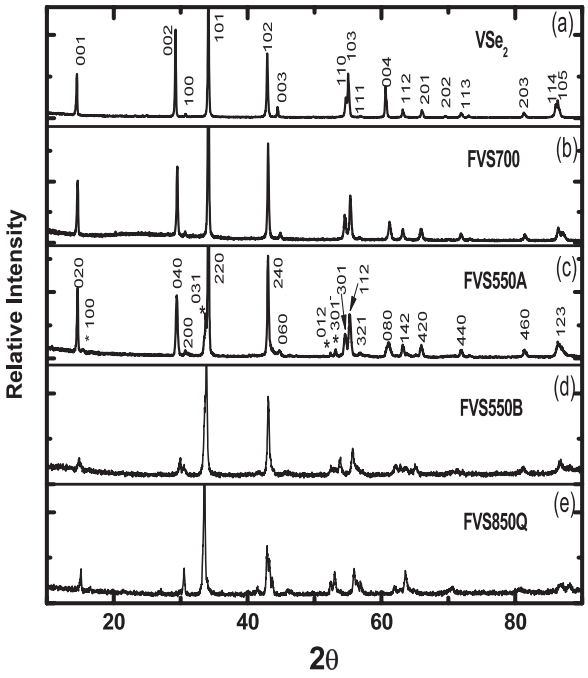

Figure 1. Powder x-ray diffraction pattern of the $Fe_{0.33}VSe_2$ compounds: (a) parent compound 1T-VSe2, (b) FVS700, prepared at 700 °C, (c) FVS550A, prepared at 550 °C, (d) FVS550B, annealed at 550 °C, and (e) FVS850Q, phase quenched from 850 °C.

3.1. Superlattice distortion

For the compound FVS550A, prepared at 550 °C, the peak positions and relative intensity of the pattern looks similar to FVS700, except for the presence of some additional weak peaks (marked by *). A careful analysis revealed a superlattice distortion of the hexagonal cell in this compound. We could index all the lines (figure 1(c)) using a monoclinic unit cell of the following dimensions:

FVS550A: $a = \sqrt{3} \times 3.364$ Å, $b = 3.527$ Å, $c = 2 \times 6.074$ Å and $\gamma = 91.609°$, $V = 249.6$ Å^3, $Z = 4$

The monoclinic cell dimensions for our $Fe_{1/3}VSe_2$ (FVS550A) compound can be compared with those reported for antiferromagnetic FeV_2Se_4 ($a = \sqrt{3} \times 3.573$ Å, $b = 3.47$ Å, $c = 2 \times 5.895$ Å and $\beta = 91.60°$, $V = 253.14$ Å^3, $Z = 4$) [10]. Although both have similar structure and the size of the cell is also the same, we found a different nature of distortion and orientation of the supercell in our compound. These differences in the detailed structural features (as yet unknown) of the Fe sublattice of the two compounds may be the reason for the considerable differences in their magnetic properties.

We should notice that a rectangular supercell (with $Z = 4$) is possible only in the case of the ordered arrangement of 1/4, 2/4 or 3/4 intercalation concentration. Hence in our $Fe_{1/3}VSe_2$ compound with 1/3 Fe atoms, the ordering can only be short range. Moreover, the crystal will be subjected to localized strains and the clustering of atoms by the accommodation of extra Fe atoms in the unit cell. These structural features will interrupt the long range ordering and are entirely consistent with the electrical and magnetic properties

around a phase transition as reported below. The irreversible effects in the magnetization processes observed below 250 K can be explained due to disordered freezing of the small number of magnetic clusters.

3.2. Long annealing and quenching

The x-ray pattern of FVS550B, which is long annealed at 550 °C for 15 d, showed significant broadening of the diffraction peaks and the absence of the lines corresponding to the 00*l* reflections of the parent phase. This pattern permitted the estimation of the approximate dimensions of the unit cell as follows:

FVS550B: $a = \sqrt{3} \times 3.44$ Å, $b = 3.45$ Å, $c = 2 \times 5.97$ Å and $\gamma = 91.74°$, $V = 245.77$ Å^3, $Z = 4$.

The reason for the substantial change in the x-ray pattern after long annealing may be related to the release of elastic strains and the changes in the short range ordering of the supercell. We observe a near absence of (00*l*) reflections and the asymmetrical broadening of (*h*0*l*) peaks, indicating that the strains are released by introducing stacking disorder in our long annealed sample. The resulting domains are now better ordered, as can be inferred from the sharp jump-like changes in the resistance and the magnetic susceptibility at the transition reported below.

In figure 1(e), we have shown the x-ray pattern of the FVS850Q phase, which is quenched from 850 °C. Though it was not possible to calculate the parameters of the unit cell of this phase from the x-ray diffraction pattern, the pattern looks very much similar to the monoclinically distorted FVS550B along with additional splitting of some of the lines.

4. Transport properties

4.1. Resistivity

We have shown the results of the measurement of the electrical resistance of the polycrystalline pellets of our compounds in figure 2. The resistivity of FVS700, FVS550A, FVS550B and FVS850Q at room temperature was found to be 1.8, 1.5, 1.3 and 0.5 mΩ cm, respectively. Except for the quenched phase FVS850Q, the others show an increase in resistance on cooling. The large resistivity and its variation by less than 20% in the temperature range 4.2–300 K indicate that these compounds have a poor metallic conduction behavior. A clear transition-like anomaly with the different extent of hysteresis can be seen on cooling in all of the phases starting at 160 K. In the quenched phase with metal-like temperature dependence, the transition anomaly appears as a small bump between the 80 and 160 K break, which is quite similar to that found for 1T-VSe_2 under pressure [16].

A minimum in the resistance is also observed at 30 K in this phase.

The largest hysteresis of the transition is found in the resistivity of FVS550A, in which a short range ordering of intercalated Fe atoms and related superlattice distortions is found by x-ray analysis. The observation of a relatively broad hysteresis from temperatures of 80 to 160 K around the

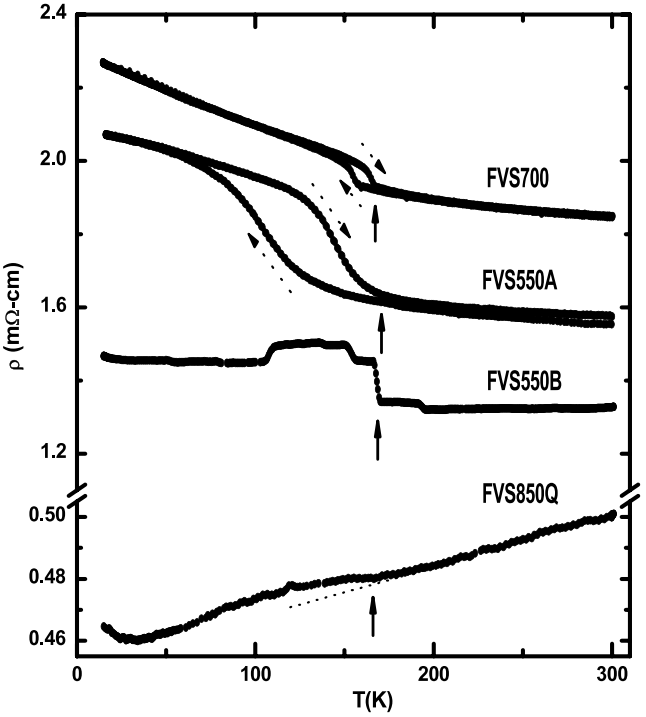

Figure 2. The temperature dependence of electrical resistivity for the different phases of $Fe_{0.33}VSe_2$ showing the onset anomaly at 160 K.

structural transition reflects that the lattice is highly strained in the FVS550A phase. This may be due to the occupancy of extra Fe atoms on the vacancy ordered sites in $Fe_{1/3}VSe_2$. At the first-order transition these local strains cause a broad hysteresis as observed in figure 2. We also notice that, after the long annealing of this phase for 15 d, the resistivity changes with the sharp jumps in the temperature range 100–160 K. The long annealing removes the lattice strains in FVS550B and so the better ordered domains exhibit a sharp transition.

4.2. Thermoelectric power

The results for the Seebeck coefficient measurements between 15 and 300 K on the sintered pellets of FVS700 and FVS550A are shown in figure 3. The Seebeck coefficient is positive and, except for the saturation effect at high temperatures, follows a metal-like temperature dependence. The overall behavior of the thermopower is very similar to the other binary and ternary sulfides of vanadium, namely $V_{1+x}S_2$ and Al_xVS_2 [17], where the transport properties along with the variation of the Hall coefficient with temperature suggest a mixed conduction behavior due to the carriers in the overlapping chalcogen p band and vanadium 3d band [12].

In contrast to the measurement on the polycrystalline samples, a very sharp jump-like anomaly was measured in the Seebeck coefficient of a good quality single-crystal flake of pure 1T-VSe_2 at its 110 K CDW transition, where the resistivity showed a relatively weak feature. This jump is, however, absent in the polycrystalline pellets of pure 1T-VSe_2 (not shown here) and also in the flakes containing a small but unknown quantity of Fe.

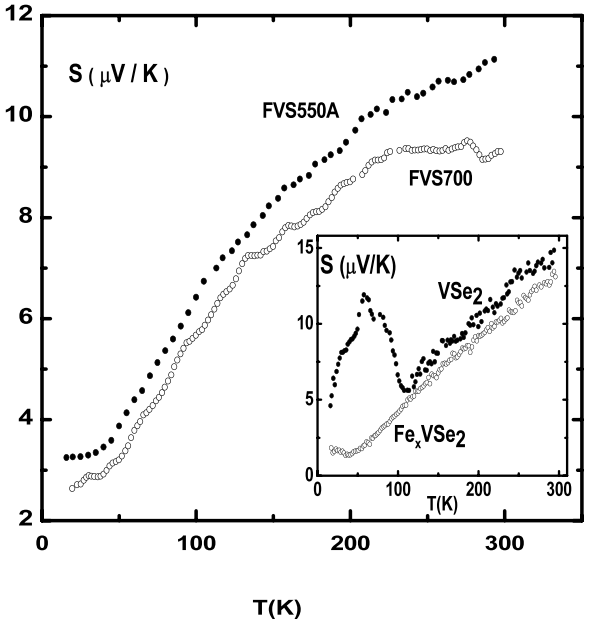

Figure 3. The Seebeck coefficient of the FVS550A and FVS700 phases, showing a saturating trend at higher temperatures. The Seebeck coefficient in the plane of VSe_2 and Fe_xVSe_2 are shown in the inset.

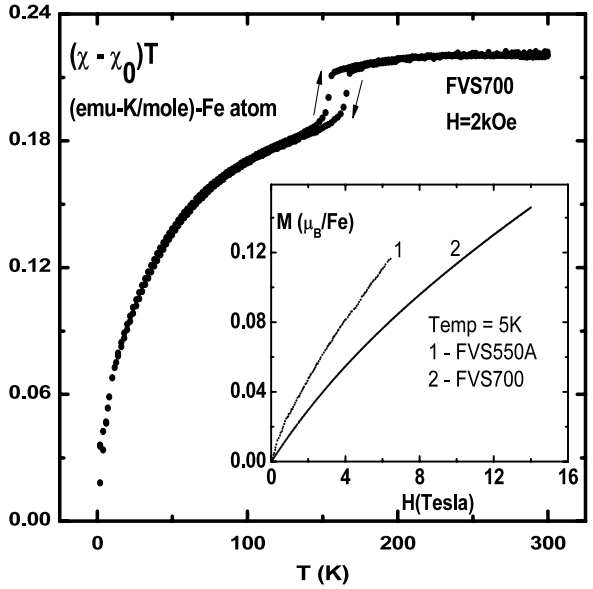

Figure 4. The plots of $(\chi - \chi_0)T$ giving temperature dependence of the Curie contribution C of Fe atoms in FVS700. A rapid reduction of C is seen below the 160 K transition. The $M(H)$ dependence of FVS700 and FVS550A at 5 K is shown in the inset.

Table 1. Magnetic parameters at room temperatures.

Phase $Fe_{1/3}VSe_2$	χ_0 (10^{-4} emu mol^{-1})	C (per mole Fe atom)	θ_w (K)	μ_{eff} (μ_B/Fe atom)
FVS700	4.7	0.23	−5	1.35
FVS550A	3.2	0.36	−8	1.7

We have plotted the Seebeck coefficient of the flakes in the inset of figure 3 for their comparison with the polycrystalline pellets of the present compounds. We can conclude that the grain boundaries in polycrystalline samples, as well as the crystal defects, eliminate the sharp variations in the thermopower at the CDW transition observed in the case of a single-crystal flake.

5. Magnetic properties

We have studied the magnetic properties of $Fe_{0.33}VSe_2$, between 2 and 300 K and up to 14 T fields. The magnetic susceptibility χ follows a $\chi = \chi_0 + C/(T - \theta_w)$ dependence around room temperature. Here χ_0 is the Pauli paramagnetic contribution (between 3.0 and 4.5 × 10^{-4} emu mol^{-1}) of the electrons in the 3d band of V atoms, and C and θ, respectively, are the Curie constant and the Weiss temperature related to the paramagnetic moments of the Fe atoms. The Curie constants for FVS700 and FVS550A were found to be 0.23 and 0.36 emu K mol^{-1} of Fe atoms that correspond to an effective magnetic moment of 1.35–1.7 μ_B/Fe-atom, respectively. Hence the Fe atoms are in the low spin state. We have reported the room temperature values of these parameters in table 1 for the two phases of $Fe_{1/3}VSe_2$, namely FVS700 and FVS550A, which were prepared at 700 and 550 °C, respectively. The low values are in contrast to the Fe moment in the intercalated Nb- and Ta-dichalcogenides and also to the corresponding compounds of V and Ti, namely FeV_2S_4, FeV_2Se_4 and $FeTi_2Se_4$ (with a Cr_3S_4 structure) [1, 6–10]. Moreover, we also find that the values of χ_0 and C in our compounds sensitively depend on the preparation conditions, as can be seen in table 1. At low temperatures the magnetic susceptibility shows characteristic deviations from the high temperature Curie–Weiss dependence. In order to clearly show this behavior we have plotted $(\chi - \chi_0)T$ versus temperature (T) of FVS700 and FVS550A, respectively, in figures 4 and 5. These plots give the temperature variation of the Curie contribution $C \sim (\chi - \chi_0)T$ of the localized moments, here we ignore the small value of the Weiss constant θ_w.

The C value in the high temperature phase of FVS700 is rather small and shows further reduction at the 160 K transition. The hysteresis in the magnetic susceptibility around this transition is very similar to the hysteresis in its resistivity as shown in figure 2. The most significant magnetic behavior is that the C value reduces continuously in its low temperature phase and attains a value of 0.015 emu K mol^{-1} of Fe atoms at 2 K temperature. Irrespective of the negative value for the Weiss constant θ_w, we found no anomalies in the susceptibility that can be related to antiferromagnetic interactions.

The results for the FVS550A phase are shown in figure 5. There are significant differences in the susceptibility behavior at high temperatures in this phase. But the rapid reduction of $C(\sim (\chi - \chi_0)T)$ at low temperatures is similar to that found for FVS700. We also plot the high field magnetization M measured for both of them in the inset of figure 4. In both cases $M(H)$ is similar and is consistent with the low value of paramagnetic susceptibility at 2 K temperature.

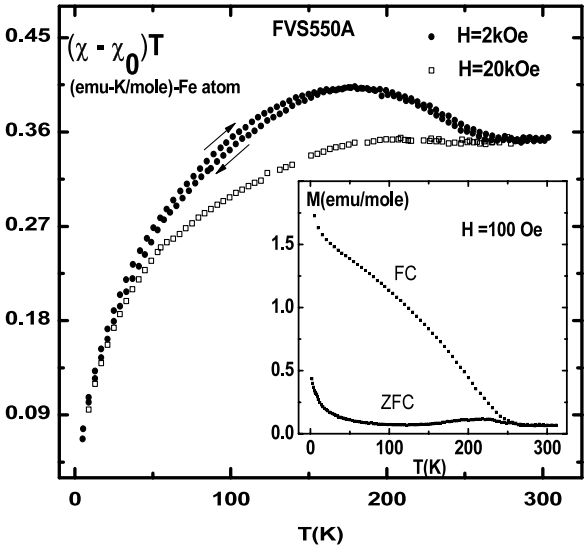

Figure 5. $(\chi - \chi_0)T$ versus temperature dependence of FVS550A found at 2 and 20 kOe. Between 50 and 250 K, χ is field-dependent. The field-cooled (FC) and zero-field-cooled (ZFC) magnetization at 100 Oe field is shown in the inset.

However, there is a marked difference in the susceptibility behavior around the 160 K transition for these two compounds, as also found in their respective resistance–hysteresis behavior (see figure 2). We relate these differences to the Fe occupancy resulting from the differently annealed conditions in the two compounds, as we have found from our already discussed x-ray diffraction studies.

At high temperatures, we see a large difference in the field-cooled (FC) and zero-field-cooled (ZFC) magnetization behavior at 100 Oe field, which starts on cooling the sample below 250 K. The FC and ZFC results are plotted in the inset of figure 5. In addition to this history-dependent magnetic behavior, we can also see in the main body of figure 5 that the susceptibility is nonlinear between 50 and 250 K, since $(\chi - \chi_0)T$ versus T plots depend upon the applied fields of 2 and 20 kOe. The irreversible and the nonlinear magnetization as shown in figure 5 are normally associated with the inhomogeneous clustering of paramagnetic centers and their freezing in random orientations upon cooling. These properties are consistent with the short range ordering and clustering of Fe atoms as inferred from our x-ray diffraction results of FVS550A.

6. Conclusion

We observed an electronic phase transition on cooling below 160 K, with varying degrees of thermal hysteresis in the electrical and magnetic properties of $Fe_{0.33}VSe_2$. This transition seems to be related to the CDW instability of the pure phases of 1T-VSe_2 at 110 K. We also find strong precursor effects of the onset of CDW much above 110 K in the electrical conductivity of good quality single-crystal flakes [12]. In our opinion the intercalation of Fe stabilizes the CDW-driven transition at a higher temperature than in pure 1T-VSe_2. Our belief can be supported by the scanning probe microscopy studies of the superlattice and CDW-related energy gap formation in the Fe-intercalated compounds of 2H-$NbSe_2$ and 2H-$TaSe_2$ [4, 5].

The nature of the CDW transition at 110 K in 1T-VSe_2 is very similar to that in 2H-$NbSe_2$ and 2H-$TaSe_2$ at 35 and 122 K, respectively. It was found in the STM studies that up to 33% intercalation of Fe in the latter compounds neither destroys the superlattice order nor the CDW-related energy gap of the host compounds [4]. In our case the CDW instability shifts to a higher temperature on Fe intercalation. The reason for this enhancement of CDW in Fe_xVSe_2 may be the reduction in the correlation effects among the conduction electrons of vanadium. A similar effect on the CDW is found by external pressure in pure 1T-VSe_2 [16]. The Fe intercalation entails a reduction in c/a and exerts a positive chemical pressure on the VSe_2 layers. The band broadening reduces correlations among electrons, thus strengthening the CDW formation at higher temperatures. We also observe that the short range vacancy ordering in the FVS550A specimen modulates the local structure but does not suppress the CDW formation. The hysteresis of the transition is much wider due to the highly strained nature of the crystal structure in this phase.

The magnetic properties of the compounds are found to be very interesting and are quite different from the other 3d intercalates of layered compounds of Nb and Ta [1, 6, 7], including FeV_2S_4, FeV_2Se_4 and $FeTi_2Se_4$ compounds [9, 10]. In contrast to these, our compounds show the absence of magnetism at low temperatures. In other compounds, all the intercalated atoms including Fe atoms respect the first Hund's rule and show magnetic moments with high spin state. In our compounds the Fe moments are unusually low and correspond to, at most, only one unpaired electron on each Fe atom. Hence the Fe, which occupies the octahedral positions in the van der Waals gap, is in the low spin state of Fe^{3+} ions, indicating that the crystal field splitting of d-levels is larger than the Hund's rule coupling energy in these compounds.

Below the CDW transition, we observe a continuous and rapid reduction in the Curie constant on cooling. There are many possible mechanisms for this variation such as the Van Vleck paramagnetic contribution, the mixed valence nature of Fe ($Fe^{3+} \leftrightarrow Fe^{2+}$), both in low spin state, or the compensation of Fe moment by the conduction electron polarization. Because of the complexity of the crystal structure and in the absence of any knowledge of the local nature of magnetism it is not possible to discuss this property. A detailed NMR or Mössbauer resonance study will be very useful to clarify the observed magnetic behavior in our compounds.

Acknowledgments

We are thankful to A K Nigam of TIFR, Mumbai and Alok Banerjee of IUC, Indore for the magnetic measurements. CSY acknowledges the Council of Scientific and Industrial Research, India for the Senior Research Fellowship grant.

References

[1] Parkin S S P and Friend R H 1980 *Phil. Mag.* B **41** 65
Parkin S S P and Friend R H 1980 *Phil. Mag.* B **41** 95

[2] Whitney D A, Fleming R M and Coleman R V 1977 *Phys. Rev.* B **7** 3405
[3] Subba Rao G V and Shafer M W 1979 *Intercalated Layered Materials* ed F Lévy (Berlin: Springer) p 99
[4] Coleman R V, Dai Z, Gong Y, Slough C G and Xue Q 1994 *J. Vac. Sci. Technol.* B **12** 1801
[5] Dai Z, Xue Q, Gong Y, Slough C G and Coleman R V 1993 *Phys. Rev.* B **48** 14543
[6] Morosan E, Zandbergen H W, Li L, Lee M, Checkelsky G, Heinrich M, Siegrist T, Ong N P and Cava R J 2007 *Phys. Rev.* B **75** 104401
[7] Eibschütz M, DiSalvo F J, Hull G W and Mahajan S 1975 *Appl. Phys. Lett.* **27** 464
[8] Hulliger F 1968 *Structure and Bonding* vol 4, ed M J Clarke *et al* (New York: Springer) p 83
[9] Morris B L, Plovnick R H and Wold A 1968 *Solid State Commun.* **7** 291
[10] Muranaka S and Takada T 1975 *J. Solid State Chem.* **14** 291
[11] Yadav C S, Naik I, Patnaik S and Rastogi A K 2004 *Proc. DAE Solid State Physics Symp.* vol 49, p 667
[12] Yadav C S and Rastogi A K 2008 arXiv:0808.1334
[13] Larson A C and Von Dreele R B 2004 General structure analysis system *Los Alomas National Laboratory Report* LAUR, 86-748
Toby B H 2001 EXPGUI *J. Appl. Crystallogr.* B **34** 210
[14] 1952 *International Tables for X-ray Crystallography* vol I, Birmingham, England
[15] Rigoult J, Guidi-Morosini C, Molini P and Thomas A 1982 *Acta Crystallogr.* B **38** 1557
[16] Friend R H, Jérome D, Schleich D M and Molinié P 1978 *Solid State Commun.* **27** 169
[17] Poddar P and Rastogi A K 2002 *J. Phys.: Condens. Matter* **14** 2689